

# Highly Efficient Nucleating Additive for Isotactic Polypropylene Studied by Differential Scanning Calorimetry

C. MARCO,<sup>1</sup> M. A. GÓMEZ,<sup>1</sup> G. ELLIS,<sup>1</sup> J. M. ARRIBAS<sup>2</sup>

<sup>1</sup> Instituto de Ciencia y Tecnología de Polímeros, C.S.I.C., Juan de la Cierva 3, 28006 Madrid, Spain

<sup>2</sup> Dirección Corporativa de Servicios Compartidos, Dirección de Tecnología de REPSOL-YPF, Embajadores 183, 28045 Madrid, Spain

Received 11 April 2001; accepted 19 September 2001

**ABSTRACT:** The influence of an organic phosphate derivative in the crystallization of the monoclinic phase of isotactic polypropylene was studied by differential scanning calorimetry. To analyze the nucleation activity of the additive, the self-nucleation process of the pure polymer was also studied by thermal techniques. A large increase in crystallization temperatures was obtained even for the lowest concentration of the additive, and its nucleating efficiency is the highest observed for  $\alpha$ -nucleating agents in isotactic polypropylene. The nucleating agent was also observed to increase the stability of the crystals formed. © 2002 Wiley Periodicals, Inc. *J Appl Polym Sci* 84: 1669–1679, 2002; DOI 10.1002/app.10546

**Key words:** polypropylene; crystallization; nucleation; differential scanning calorimetry

## INTRODUCTION

Crystallization occurs when a polymer is cooled well below its melting temperature, and the phase transformation that takes place can be described by a nucleation and growth mechanism. Nucleation is the process by which a new crystalline phase is initiated and the nuclei can be formed either homogeneously or heterogeneously. Homogeneous nucleation originates from statistical fluctuations of the polymer chains in the melt and takes place at a constant rate. In contrast, heterogeneous nucleation is caused by the presence of heterogeneities that induce the development of crystallinity and the rate of nucleation is

variable. These heterogeneities can be impurities, residual polymer crystals, as in the case of the self-nucleation process, or specific substances that may act as nucleating agents.

Isotactic polypropylene (iPP) has a very complex structural behavior and can crystallize in four different crystal forms<sup>1–8</sup>:  $\alpha$  (monoclinic),  $\beta$  (hexagonal),  $\gamma$  (triclinic), and smectic. The  $\alpha$  form is the thermodynamically stable crystalline modification and is that usually obtained under common processing conditions. In iPP, the crystallization process is controlled by nucleation.<sup>9</sup> In the region of crystallization where heterogeneous nucleation occurs, this process can be improved by the addition of specific additives or nucleating agents which shorten the induction time of crystallization of a given polymer, providing foreign surfaces or nuclei that reduce the free energy of formation of a new polymer nucleus.<sup>10</sup> They are commonly used in the polymer industry to shorten injection-molding cycle times, thus reduc-

Correspondence to: C. Marco (cmarco@ictp.csic.es).

Contract grant sponsor: CICYT; contract grant number: MAT98-0914; contract grant sponsor: CAM; contract grant sponsor: 07N/0032/1999.

*Journal of Applied Polymer Science*, Vol. 84, 1669–1679 (2002)  
© 2002 Wiley Periodicals, Inc.

ing production costs, generating smaller spherulites, and thus improving the optical and mechanical properties, as is the case for iPP.<sup>11</sup> A large number of compounds were reported to nucleate the  $\alpha$  form of iPP,<sup>10–14</sup> and several others act as nucleating agents of the  $\beta$  form,<sup>15–27</sup> depending on the dispersion and concentration of the additives and the cooling rates.

The established method to evaluate nucleating agent efficiency is to determine either the crystallization temperature of the nucleated system in a dynamic DSC experiment, or the time needed to reach a given crystallization transformation in an isothermal DSC experiment, and to compare these with the same parameter obtained for the polymer without additives. Fillon et al.<sup>28,29</sup> have developed a method to determine this efficiency considering the nonnucleated system as the lower limit, and a wholly self-nucleated polymer as the upper limit of the nucleation efficiency scale. The best  $\alpha$ -nucleators reported for iPP have efficiencies in the 50–66% range,<sup>28,29</sup> and dibenzylidene sorbitol, which is commonly used to significantly increase transparency in iPP, has an efficiency of 40%, far removed from optimum performance that would correspond with wholly self-nucleated polypropylene (PP).

As part of a broad project related to the development of transparent and high-modulus materials based on PP, this article presents a study of the nucleating efficiency of a new organic phosphate derivative in the crystallization process of the monoclinic phase of iPP. The nucleating efficiency was evaluated by using differential scanning calorimetry, and the influence of the concentration of the nucleating agent and the thermal treatments were analyzed. To determine the upper limit of the nucleation efficiency scale, the self-nucleation process in our pure iPP sample has also been investigated.

## EXPERIMENTAL

### Materials

The iPP sample used in this study is a commercial grade supplied by REPSOL-YPF (Madrid, Spain) with an isotacticity of 95% as determined by solution NMR. The viscosity average molecular weight was obtained by intrinsic viscosity measurements by using a modified Ubbelohde viscometer in decalin solutions at 135°C. A concentration of 0.1 g dL<sup>-1</sup> was used, and the mea-

surements were carried out under nitrogen atmosphere. The intrinsic viscosity–molecular weight relationship is given by<sup>30</sup>:

$$[\eta] = 1.10 \times 10^{-4} M_v^{0.80}$$

The intrinsic viscosity was found to be 1.64 dL g<sup>-1</sup> and the calculated  $M_v$  was 164,000.

The nucleating agent used is methylenebis(4,6-di-*tert*-butylphenyl) phosphate sodium salt, ADK STAB NA 11 UH, provided by Asahi Denka Kogyo K.K. (Tokyo, Japan), which we will call NA11.

The dispersion of the nucleating additive in the polymer was achieved by melt blending in a twin-screw extruder (MP 2030) (APV Baker, Peterborough, UK) at a rotor speed of 150 rpm. The concentration of NA11 was between 0.05 and 0.5 wt %. To incorporate such a small concentration of the nucleating additive, a compound of the nucleating agent and the iPP powder, obtained by cryogenic grinding, was previously prepared.

### Physical Properties

The thermal stability of all samples was studied by thermogravimetric analysis by using a Mettler TA-4000/TG-50 thermobalance in an oxygen atmosphere and at a heating rate of 20°C min<sup>-1</sup>.

The thermal properties were analyzed under dynamic conditions in a Perkin–Elmer DSC-7/7700/UNIX differential scanning calorimeter (DSC), calibrated with indium ( $T_m = 156^\circ\text{C}$ ,  $\Delta H_m = 28.45 \text{ J g}^{-1}$ ). The experiments were carried out in a nitrogen atmosphere by using 10–12 mg of sample sealed in an aluminum pan. The transition temperatures were taken as the peak maxima in the calorimetric curves. The degree of crystallinity ( $1 - \lambda$ ) was calculated from the ratio  $\Delta H_a/\Delta H_u$ , where  $\Delta H_a$  and  $\Delta H_u$  are the apparent and the completely crystalline heats of fusion, respectively. For  $\Delta H_u$ , the value of 177.0 J g<sup>-1</sup> was used.<sup>31</sup>

The self-nucleation experiments in pure iPP were performed by using four thermal steps, described later.

Crystallization experiments under dynamic conditions were carried out on pure iPP and the nucleated systems by cooling to 40°C at cooling rates of 1, 2, 5, 10, and 20°C min<sup>-1</sup>, after melting the samples at 210°C for 10 min. All samples were heated to 210°C at 10°C min<sup>-1</sup> after crystallization.

X-ray diffractograms of the samples at room temperature were obtained by using a Rigaku Geigerflex-D/max X-ray diffractometer fitted with a Rigaku RU-200 rotating anode generator, at  $1^\circ \text{min}^{-1}$  in a  $2\theta$  range between  $5$  and  $35^\circ$  using Ni-filtered  $\text{CuK}\alpha$  radiation. Samples were prepared as films by compression molding with thermal histories identical to those investigated by DSC.

## RESULTS AND DISCUSSION

Prior to the investigation of the thermal behavior, the thermal stabilities of all the materials were determined under more drastic conditions than the DSC experiments (i.e., in an oxygen atmosphere). An initial degradation temperature of  $243^\circ\text{C}$  was obtained for NA11 and  $225^\circ\text{C}$  for pure iPP, both well above the melting temperature used in this work. The thermal stabilities of the nucleated systems were similar to that of pure iPP, which indicated that blending does not affect the stability of the PP matrix.

To select the thermal history to be imposed on the samples prior to the determination of the rates of crystallization, melt-phase memory effects were considered, because the crystallization rate is highly conditioned by the thermal history. At the beginning of the crystallization process, the nuclei present in the system are heterogeneous nuclei, formed by particles chemically different from the crystallizing polymer, and athermal homogeneous nuclei. Although the heterogeneous nuclei are hardly affected by the thermal history of the melt, the concentration of athermal homogeneous nuclei (i.e., residual polymer crystal fragments left from previous structures) is very dependent on the melting temperature and melting time.<sup>32,33</sup> The influence of the melting temperature and residence time in the melt on the crystallization rate was investigated at a given isothermal crystallization temperature. The kinetic crystallization parameter used to monitor this effect was the time needed to reach 10% of the crystalline transformation,  $\tau_{10}$ , obtained from the partial integral of the corresponding DSC crystallization exotherm. A crystallization temperature of  $128^\circ\text{C}$  was used because the development of crystallinity at this temperature takes place at intermediate transformation times. Thus, experimental problems related to the rapid development of crystallinity at very large undercoolings, or difficulties in the determination of the DSC

baseline at extremely long transformation times at high crystallization temperatures, are eliminated. The heating rate applied to reach the melt temperature was  $200^\circ\text{C min}^{-1}$  to limit the presence of residual nuclei in the melt.<sup>33,34</sup>

When the influence of the melt temperature at a fixed time of 10 min and at several crystallization temperatures was analyzed, an increase in  $\tau_{10}$  was observed with melt temperature up to a temperature of  $210^\circ\text{C}$ , from which  $\tau_{10}$  remained constant. The influence of the residence time at different melt temperatures was also analyzed and it was observed that by increasing the time the sample remained in the melt at a constant temperature, the crystallization time  $\tau_{10}$  increased, indicating a gradual reduction of the number of athermal nuclei. At high-melt temperatures,  $210$ – $230^\circ\text{C}$ , the values of  $\tau_{10}$  were almost constant for residence times of 10 min and longer, because the initial number of athermal nuclei is relatively low. However, at lower melt temperatures, closer to the melting point of iPP, for example,  $190^\circ\text{C}$ , a much higher number of athermal nuclei are initially present. In this case, with increasing residence time in the melt,  $\tau_{10}$  was seen to increase as the number of athermal nuclei decreased, even for the longest residence times, demonstrating the importance of the contribution of the athermal nuclei to the crystallization rates.

These results are in perfect agreement with those described by Alfonso and Ziabicki<sup>33</sup> and Carfagna et al.,<sup>34</sup> but contradict those of Janimak et al.,<sup>35</sup> who did not observe any dependence of crystallization rates on melting thermal history in isothermal crystallization studies. From these results, a thermal history of melting at  $210^\circ\text{C}$  for 10 min, after heating at  $200^\circ\text{C min}^{-1}$ , was selected to investigate the nonisothermal crystallization of the iPP sample and the nucleated systems in the absence of melt-phase memory effects.

Given that crystallization depends on the molecular characteristics and the thermal history imposed, prior to the study of the crystallization behavior of all the samples and the evaluation of the efficiency of the nucleating additives, we have evaluated the self-nucleation of the iPP used in this study, as this must be analyzed for each particular sample as has been previously established.<sup>28</sup> Self-nucleation in polymers was first introduced by Blundell et al.<sup>36</sup> to describe the nucleation of chain-folded crystals in solution by crystal fragments of high-molecular weight present in the same solution. Now, the term self-nucleation is generally applied to describe nucle-

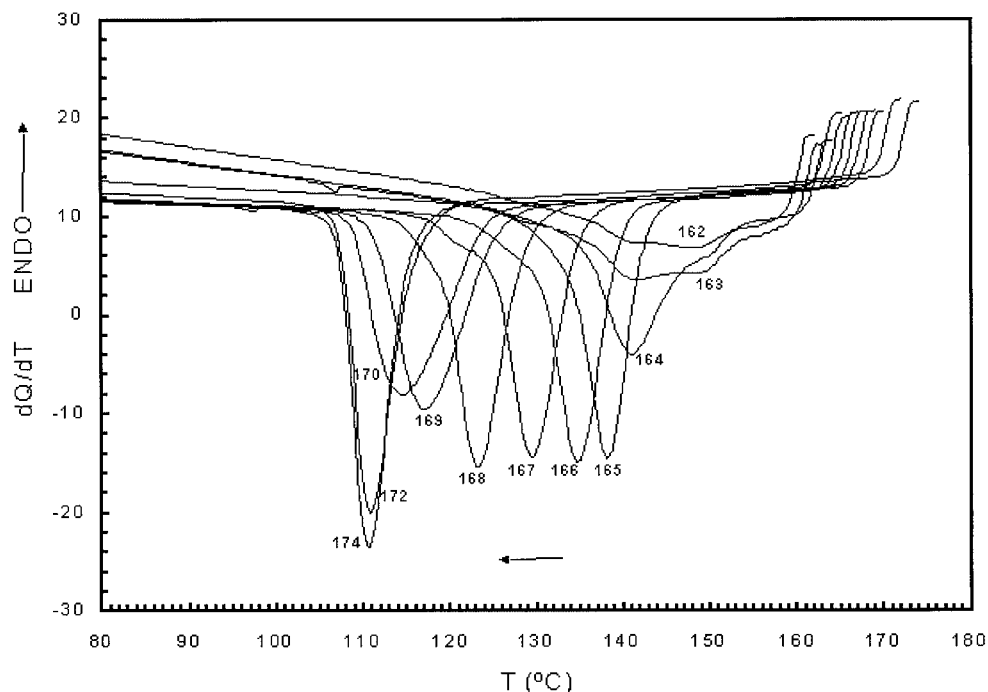


**Figure 1** Crystallization exotherms of iPP cooled at  $10^{\circ}\text{C min}^{-1}$  after partial melting at indicated values of  $T_s$ .

ation of polymers in the melt or in solution induced by previously produced polymer crystals. Self-nucleation phenomena can be generated in DSC by using four thermal steps, which correspond to<sup>28,29,37</sup> (1) erasure of previous thermal history; (2) creation of a crystalline state in pre-determined dynamic or isothermal conditions; (3) partial melting at a temperature located in the melting range,  $T_s$ ; and (4) isothermal or dynamic crystallization.

The experimental conditions used to generate self-nucleation in our iPP sample are described below. In step 1, to eliminate the melt-phase memory effects the sample was held at  $210^{\circ}\text{C}$  during 10 min. Step 2 comprised an isothermal crystallization at  $128^{\circ}\text{C}$  for 45 min after cooling from the melt at  $64^{\circ}\text{C min}^{-1}$ . In step 3, which is the essential step in self-nucleation, the samples were heated at  $10^{\circ}\text{C min}^{-1}$  to values of  $T_s$  selected between  $175$  and  $160^{\circ}\text{C}$  and maintained at these temperatures for 5 min. In step 4, a dynamic crystallization was carried out, cooling the samples to  $40^{\circ}\text{C}$  at  $10^{\circ}\text{C min}^{-1}$ . The subsequent heating process, at  $10^{\circ}\text{C min}^{-1}$  to  $210^{\circ}\text{C}$ , was also investigated. The crystallization exotherms obtained under dynamic conditions after partial melting at different values of  $T_s$  are shown in Figure 1. When  $T_s$  is located in the upper part of

the melting range known as region II,  $165^{\circ}\text{C} \leq T_s \leq 170^{\circ}\text{C}$ , a decrease of the crystallization temperatures is observed as  $T_s$  increases. This behavior is related to a drastic reduction of the nucleation density because of a decrease in the concentration of remaining crystalline fragments. In contrast, when melting takes place at  $T_s > 170^{\circ}\text{C}$ , located at the end of the melting endotherm, region I, the number of nuclei remain minimal and constant, and the crystallization occurs at the same temperature. The crystallization behavior when the sample is melted at  $T_s < 165^{\circ}\text{C}$ , which corresponds to region III in the lower part of the melting endotherm, is rather complex. A double exotherm is observed with a large reduction of the material that has recrystallized. It is clear that the melting process is incomplete and only the smaller and imperfect crystals are melted, whereas the others may experience an annealing process during heating.

The heating of the samples after the recrystallization process described above is shown in Figure 2. In the iPP samples which have been partially melted at  $T_s < 165^{\circ}\text{C}$ , two endothermic peaks are observed, one at high temperature located at  $172$ – $176^{\circ}\text{C}$  and the other at temperatures below  $170^{\circ}\text{C}$ . The low-temperature peak corresponds to the melting of crystals formed dur-

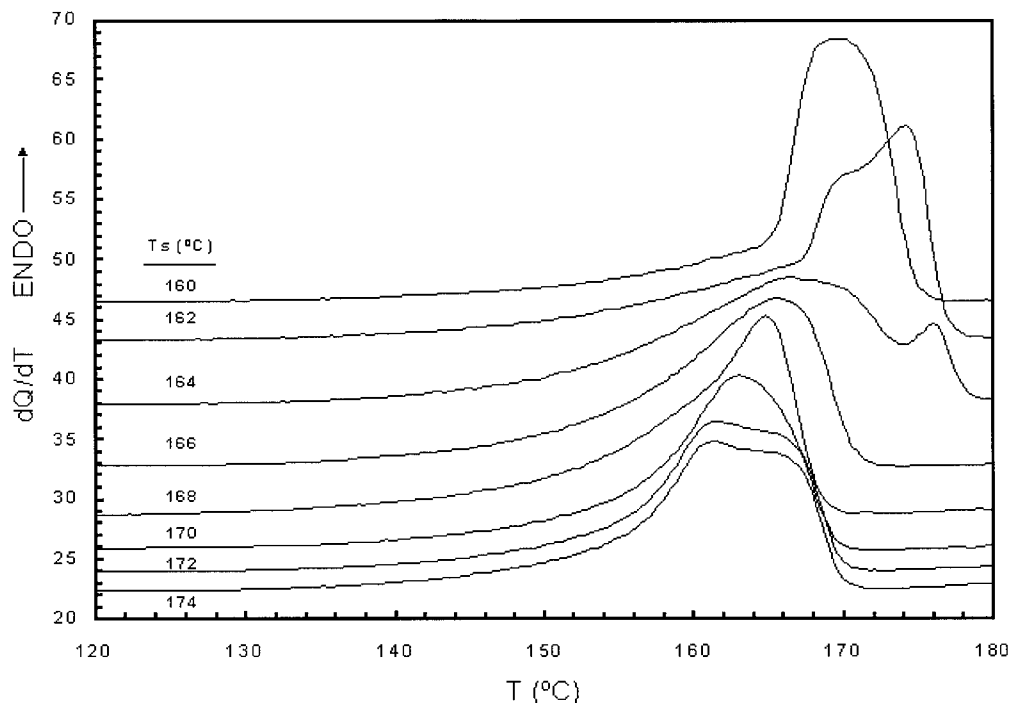


**Figure 2** Melting endotherms of iPP heated at  $10^{\circ}\text{C min}^{-1}$  after the recrystallization process in Figure 1.

ing the cooling process. However, the peak at high temperatures can be associated with those crystals that have not melted at  $T_s < 165^{\circ}\text{C}$ , and experience an increase in their crystal sizes because of an annealing process on heating. When  $T_s$  increases, but is still in region III, the intensity of the higher temperature endotherm decreases because the concentration of crystals which may be annealed is smaller, but the temperature of the peak is higher because the annealing takes place at high temperatures, as was previously observed by Fillon et al.<sup>28</sup> When the conditioning time at fixed  $T_s$  is increased, the temperature of the high-temperature endotherm increases, as can be observed in Figure 3. This behavior confirms that an annealing process generates this endotherm.

The double peak observed in the crystallization and melting can be explained by modifications of the monoclinic structure of iPP during the annealing process, and two phases  $\alpha_1$  and  $\alpha_2$  have been described.<sup>38</sup> Phase  $\alpha_1$  is generated during the cooling process, whereas phase  $\alpha_2$  is that formed at high temperature with higher melting temperature. This phase is probably generated from the nuclei produced during the self-nucleation experiment. It is evident that the crystallization temperature obtained during the self-nucleation process is completely dependent on the

conditioning temperature where the partial melting has been performed,  $T_s$ . At values of  $T_s > 170^{\circ}\text{C}$ , a constant crystallization temperature was obtained, considered the crystallization temperature of the non-nucleated iPP. For values of  $T_s$  in the interval between 165 and  $170^{\circ}\text{C}$ , a self-nucleation process is generated and the crystallization temperature decreases with  $T_s$ , reaching a maximum value of  $140^{\circ}\text{C}$ . This temperature is considered the crystallization temperature of the best self-nucleated sample. When  $T_s$  is below  $165^{\circ}\text{C}$ , the self-nucleation process competes with an annealing process that becomes more important as  $T_s$  and the conditioning time increase.

The evolution of the crystallization temperatures and their corresponding enthalpies, and melting temperatures with  $T_s$ , is shown in Figure 4. In region I, crystallization temperatures and enthalpies are constant, and the crystals formed at the lowest crystallization temperatures are the smallest and melt at very low temperatures (i.e., at  $160^{\circ}\text{C}$ ). These imperfect crystals experience a melting-recrystallization-melting process on heating which generates a second endotherm at  $165\text{--}166^{\circ}\text{C}$  (see Fig. 2). In region II, as previously mentioned, the crystallization temperatures increase with a slight increase in enthalpy when  $T_s$  decreases. A single endotherm is observed between  $163$  and  $166^{\circ}\text{C}$  as



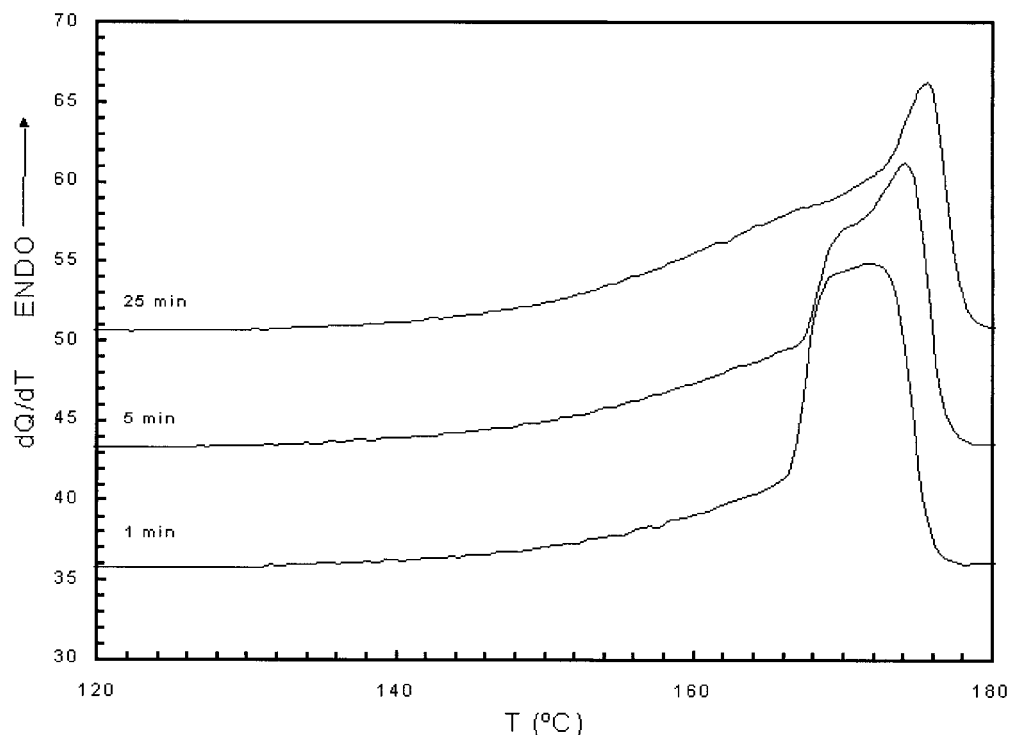


**Figure 3** Melting endotherms of iPP heated at  $10^{\circ}\text{C min}^{-1}$  after partial melting at  $162^{\circ}\text{C}$  at the conditioning times indicated, and recrystallization on cooling at  $10^{\circ}\text{C min}^{-1}$ .

$T_s$  increases. In region III, the crystallization enthalpies decrease with  $T_s$ , and a double exotherm and endotherm are observed because of a predominant annealing process instead of self-nucleation, as explained above.

The crystallization behavior of the nucleated iPP/NA11 systems were studied by DSC under dynamic conditions and their corresponding exotherms are shown in Figure 5. The crystallization temperatures increase with increasing concentration of the nucleating agent and depend strongly on the cooling rate. Figure 6 shows the changes in the crystallization temperatures for different cooling rates. It can be clearly observed that for all cooling rates the crystallization temperature increases relative to the value of iPP without nucleating agent. This increase is spectacular for the lowest concentration of the additive (i.e., of 0.05%) and continues to increase, although at a lower rate for higher concentrations. At the highest concentration of NA11 studied, an increment of  $21^{\circ}\text{C}$  in the crystallization temperature is observed, much higher than that previously reported in the literature for this nucleating agent.<sup>39</sup> The samples crystallized under dynamic conditions at different cooling rates were studied

by X-ray diffraction at room temperature. The diffractograms of all systems corresponded to the  $\alpha$  form of iPP with the characteristic reflections of the monoclinic structure, as shown in Figure 7(b), together with the crystalline structure of the nucleating agent [Fig. 7(a)].

The increase in crystallization rates induced by the nucleating agent NA11 is also reflected in the increase in concentration of crystalline nuclei, as shown in Figure 8. The progress of the spherulitic growth at a cooling rate  $1^{\circ}\text{C min}^{-1}$  of nonnucleated iPP is shown in Figure 8(a–d) at temperatures between  $128$  and  $121^{\circ}\text{C}$  and is compared with the dense spherulitic morphology observed for nucleated iPP with 0.05% NA11 at  $137^{\circ}\text{C}$  cooled at the same rate [Fig. 8(e)]. It is important to point out that the nucleation density increases with addition of the nucleating agent because the nucleation rate becomes more predominant than the spherulitic growth rate, resulting in an increase in the overall rate of crystallization, which leads to smaller spherulites. When the size of the spherulites is smaller than the wavelength of light, there is no refraction and the transparency of the material is improved. The increase in nucleation density and the consequent increase in

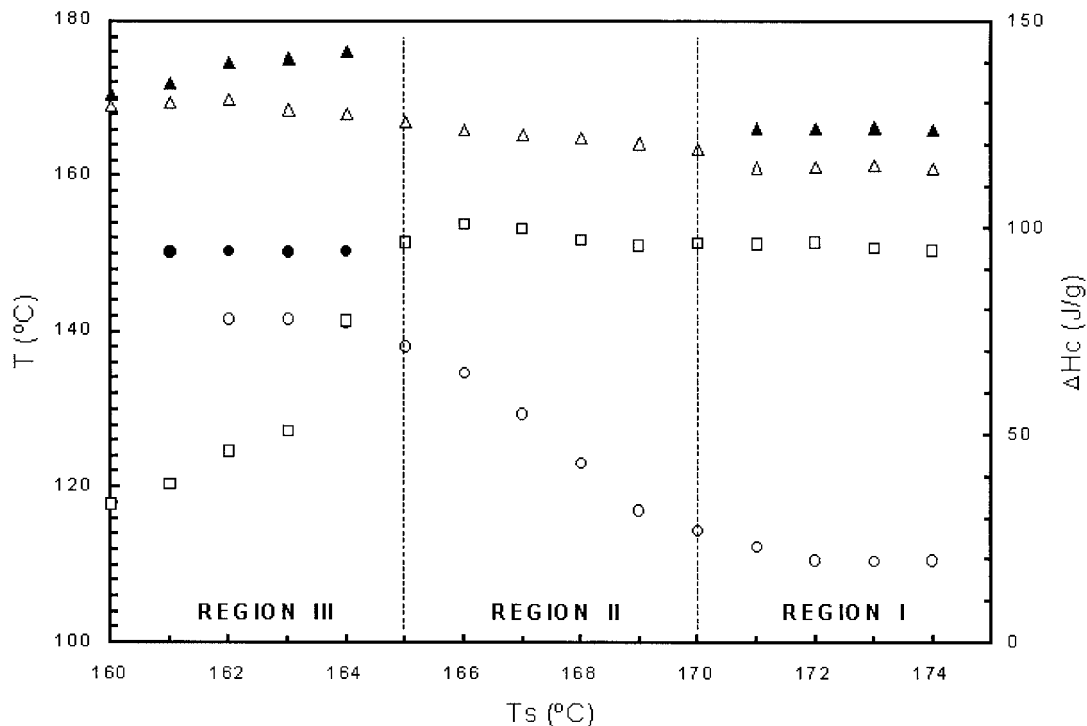


**Figure 4** Variation of crystallization temperatures (○, ●) and crystallization enthalpies (□) obtained on cooling at 10°C min<sup>-1</sup>, and melting temperatures (△, ▲) of the subsequent heating curves, as a function of the partial melting temperature,  $T_m$ .

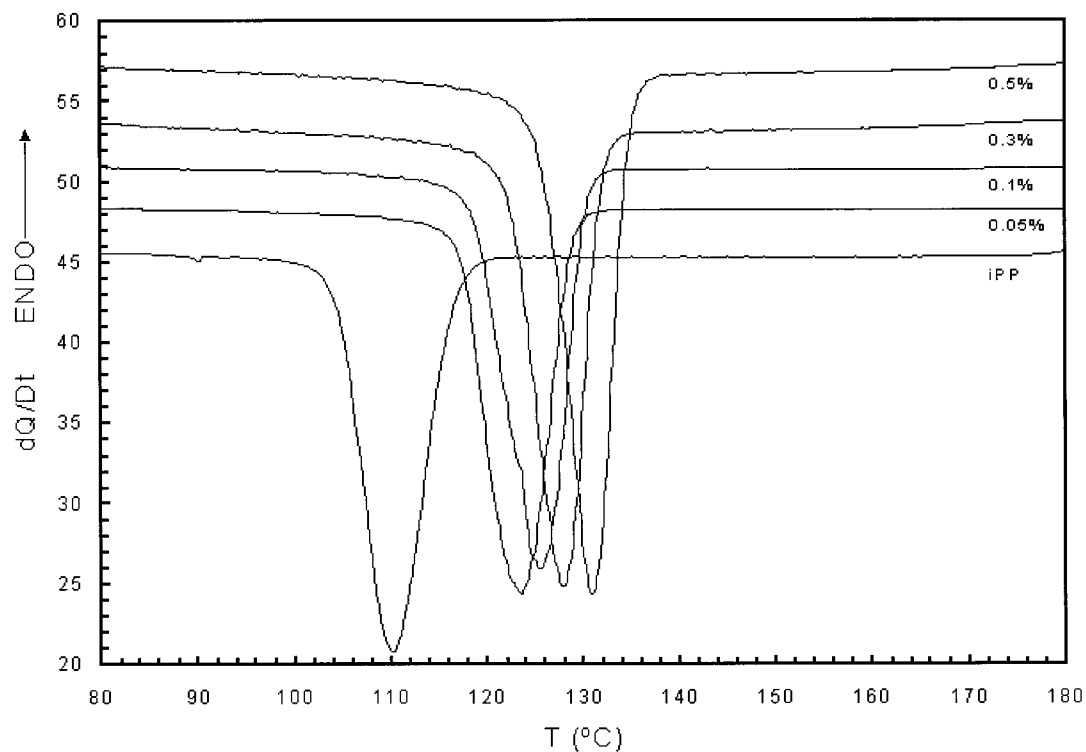


**Figure 5** Crystallization exotherms of iPP/NA11 cooled at 10°C min<sup>-1</sup> for the additive concentrations indicated.

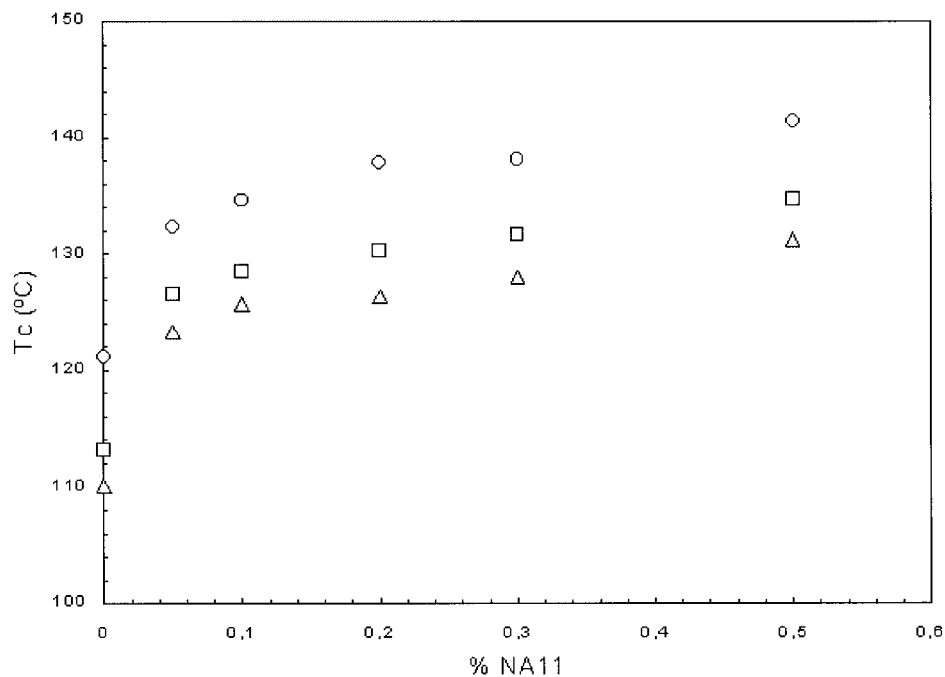


**Figure 6** Variation of crystallization temperatures with concentration of NA11 at different cooling rates: (○) 1°C min<sup>-1</sup>, (□) 5°C min<sup>-1</sup>, (△) 10°C min<sup>-1</sup>.

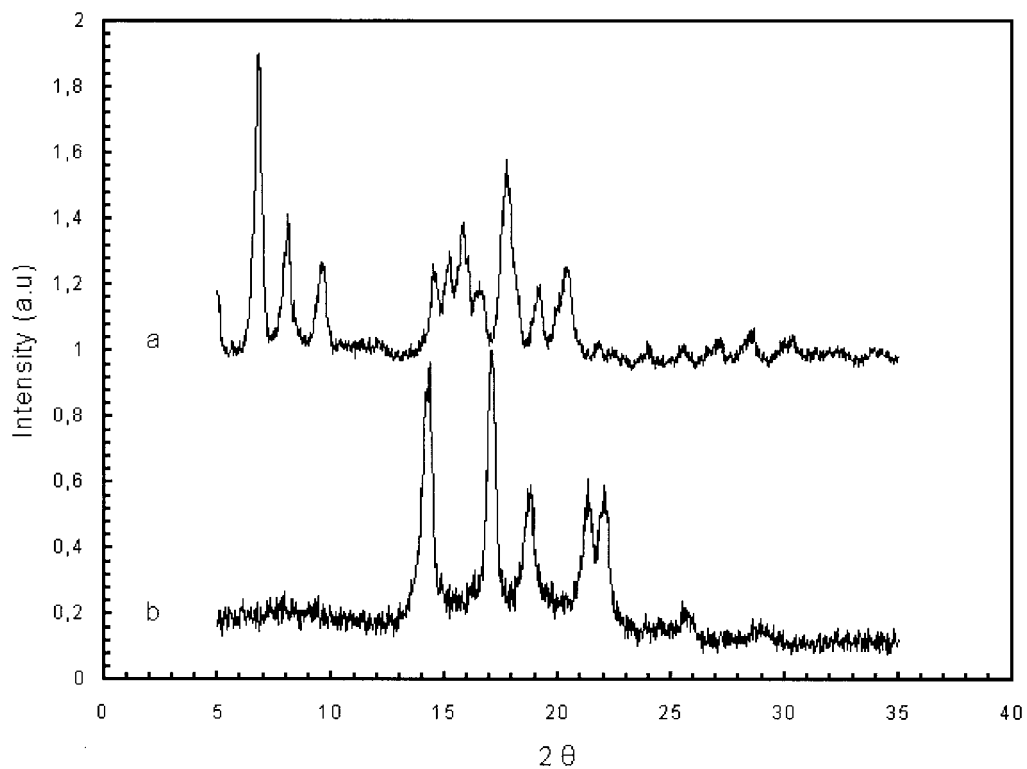


**Figure 7** X-ray diffractograms of (a) pure NA11 and (b) iPP with 0.1% NA11, recorded at room temperature.



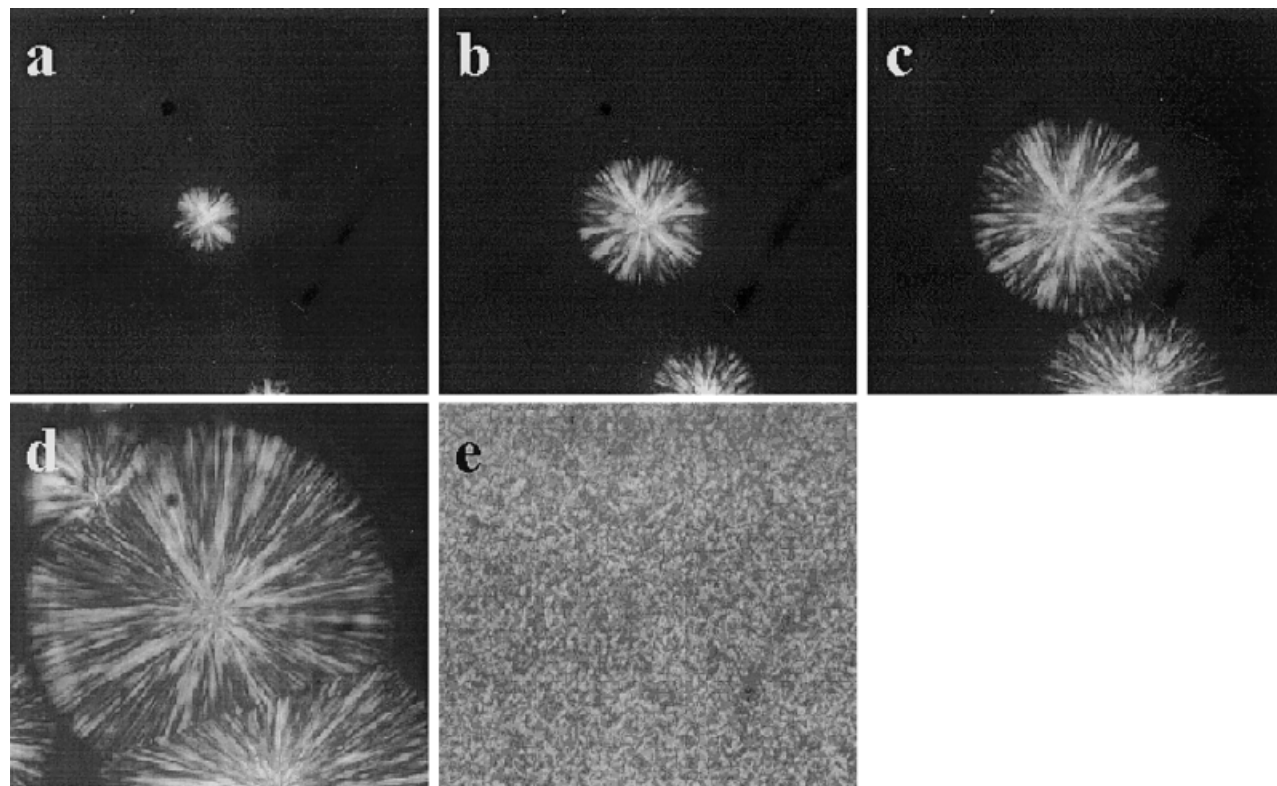


**Figure 8** Optical micrographs of the crystallization process on cooling at  $1^{\circ}\text{C min}^{-1}$  for pure iPP at (a)  $128^{\circ}\text{C}$ , (b)  $126^{\circ}\text{C}$ , (c)  $124^{\circ}\text{C}$ , (d)  $121^{\circ}\text{C}$ , and (e) for iPP/NA11 0.05% at  $137^{\circ}\text{C}$ .

the concentration of crystalline entities produced correlates with an increase in crystallization enthalpies when the concentration of the nucleating agent is incremented and the cooling rate reduced. A maximum value of 62% is obtained for the crystallinity of the nucleated systems compared to 52% for the nonnucleated iPP, at a cooling rate of  $1^{\circ}\text{C min}^{-1}$ . This increment in crystallinity reduces the material's flexibility, producing an increase in the flexural modulus and tensile strength, as will be demonstrated elsewhere.<sup>40</sup>

As previously mentioned, a method used to calculate the nucleating efficiency of an additive considers the best nucleated polymer as that obtained by a self-nucleation process.<sup>28,29,36,41,42</sup> The presence of crystal fragments in the melt of iPP, produced by a self-nucleation process, can act as an ideal nucleating agent because the concentration, dispersion, and interactions are the best that can be achieved between the additive and the matrix. The method considers the non-nucleated sample and the best self-nucleated sample as the two extreme limits of the efficiency scale for a particular polymer. The nucleating efficiency,  $NE$ , varies from 0 to 100 and is given by:

$$NE = 100 (T_c - T_{c1}) / (T_{c2 \max} - T_{c1}) \quad (1)$$

where  $T_{c1}$  and  $T_{c2 \max}$  are the crystallization temperatures of the non-nucleated and the self-nucleated polymer, respectively.<sup>42</sup> A value of  $140^{\circ}\text{C}$  was used for  $T_{c2 \max}$  obtained from the self-nucleation experiments, and the calculated nucleation efficiency for a nucleated system with a 0.5% concentration of NA11 was 71%. This efficiency is higher than any value reported for nucleating additives in iPP, which vary for the  $\alpha$ -nucleators from 50 to 66%.<sup>29</sup>

Finally, the melting behavior of all the nucleated systems was also analyzed. The heating of samples crystallized under dynamic conditions at different cooling rates showed two endotherms for nonnucleated iPP with peak maxima very dependent on cooling and heating rates. However, in the nucleated systems the endotherm at lower temperature is hardly observable and the endotherm at high temperature is observed in the range between  $164$  and  $170^{\circ}\text{C}$ , as previously reported,<sup>43</sup> although some authors have observed a double melting peak in nucleated systems.<sup>44</sup> Figure 9 shows the heating DSC curves of non-

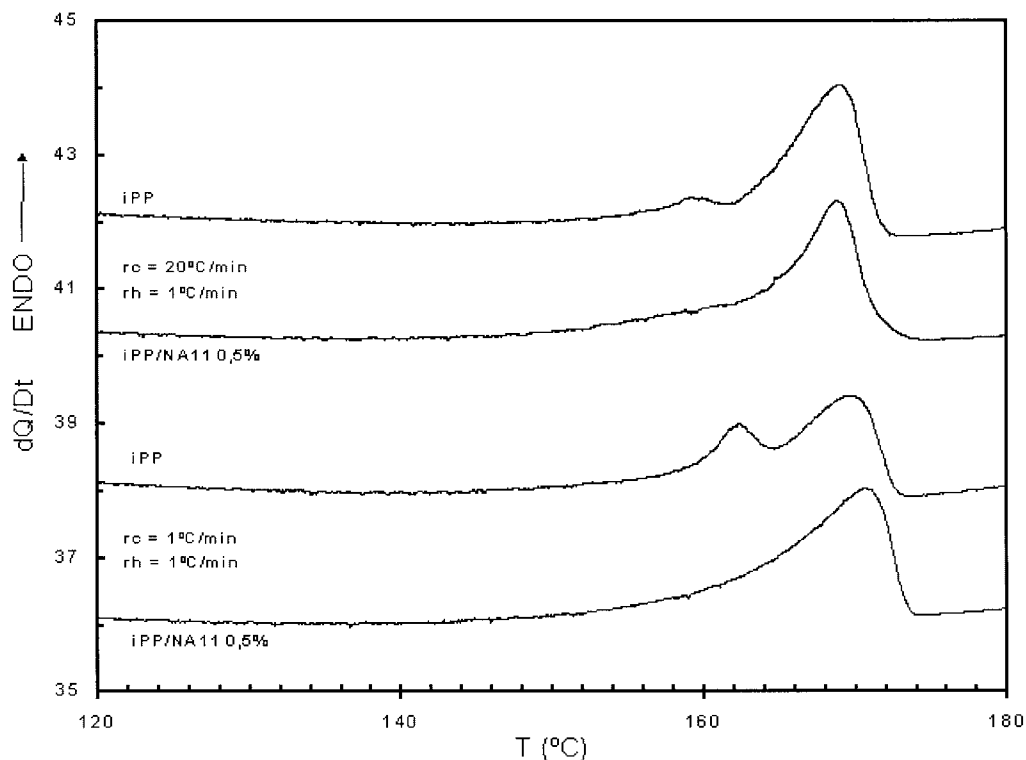


**Figure 9** Melting endotherms of iPP and iPP/NA11 0.5% at the heating and cooling rates indicated.

nucleated iPP and a nucleated iPP sample with 0.5% NA11. In the absence of different crystalline forms, the observation of multiple melting endotherms in isotactic PP was assigned to the existence of two different spherulitic structures,<sup>45</sup> different crystal sizes,<sup>46</sup> and recrystallization and reorganization of the imperfect monoclinic crystals during heating.<sup>47,48</sup> In our study the formation of the  $\beta$ -form was excluded from the results of the X-ray diffraction experiments. Therefore, the double endotherm observed in pure iPP is due to a melting-recrystallization-melting process of the iPP crystals. In the nucleated systems these crystals are formed at much higher temperatures and only one endotherm is observed in the DSC curves even at very low heating rates ( $1^\circ\text{C min}^{-1}$ ). The nucleating additives used, while they increase the crystallization temperature, reduce the tendency of the crystals to recrystallize (i.e., increase the stability of the crystals formed).

## CONCLUSION

The nucleation efficiency of the organic phosphate derivative analyzed in the crystallization of the  $\alpha$

phase of isotactic PP is the highest value obtained when compared with previously reported data. The effect of the nucleating agent on the crystallization temperature of iPP is very important at a very low concentration of the additive (i.e., 0.05%). This increase in crystallization rate continues smoothly for the higher additive contents investigated. Differences in the melting behavior of the nucleated and nonnucleated polymer were determined, demonstrating an increase in stability of the crystals formed in the nucleated polymers, reducing the incidence of reorganization on heating.

The authors thank C. Blancas (REPSOL-YPF) and M. A. López Galán (ICTP) for collaboration. Financial support from the following research projects is gratefully acknowledged: CICYT (MAT98-0914) and CAM (07N/0032/1999).

## REFERENCES

1. Padden, F. J.; Keith, H. D. *J Appl Phys* 1959, 30, 1479.
2. Keith, H. D.; Padden, F. J.; Walter, N. M.; Wyckokk, H. W. *J Appl Phys* 1959, 30, 1485.

3. Natta, G.; Corradini, P. *Nuovo Cimento Soc Ital Fis, A* 1960, 15, 40.
4. Turner-Jones, A.; Aizlewood, J. M.; Beckett, D. R. *Makromol Chem* 1964, 75, 134.
5. Norton, D. R.; Keller, A. *Polymer* 1985, 26, 704.
6. Meille, S. V.; Brückner, S.; Porzio, W. *Macromolecules* 1990, 23, 4114.
7. Varga, J. *J Mater Sci* 1992, 27, 2557.
8. Meille, S. V.; Ferro, D. R.; Brückner, S.; Lovinger, A. J.; Padden, F. J. *Macromolecules* 1994, 27, 2615.
9. Mandelkern, L. in *Comprehensive Polymer Science. The Synthesis, Characterization, and Applications of Polymers*; Allen, G., Bevington, J., Eds., Polymer Properties; Pergamon Press: New York, 1989; Vol. 2.
10. Wunderlich, B. *Macromolecular Physics, Vol. 2: Crystal Nucleation, Growth, Annealing*; Academic Press: New York, 1976; p 44.
11. Beck, H. N. *J Appl Polym Sci* 1967, 11, 673.
12. Binsbergen, F. L.; de Lange, B. G. M. *Polymer* 1970, 11, 309.
13. Menczel, J.; Varga, J. *J Therm Anal* 1983, 28, 161.
14. Kowalewski, T.; Galeski, A. *J Appl Polym Sci* 1989, 32, 2919.
15. Garbarczyk, J.; Paukszta, D. *Colloid Polym Sci* 1985, 263, 985.
16. Jacoby, P.; Bersted, B. H.; Kissel, W. J.; Smith, C. E. *J Polym Sci, Polym Phys Ed* 1986, 24, 461.
17. Liu, J.; Wei, X.; Guo, Q. *J Appl Polym Sci* 1990, 4, 2829.
18. McGenity, P. M.; Hooper, J. J.; Payntes, C. D.; Rilley, A. M.; Nutbeem, C. K.; Elton, N. J.; Adams, J. M. *Polymer* 1992, 33, 5215.
19. Stocker, W.; Schumacher, M.; Graff, S.; Thierry, A.; Wittmann, J. C.; Lotz, B. *Macromolecules* 1998, 31, 807.
20. Bauer, T.; Thomann, R.; Mülhaupt, R. *Macromolecules* 1998, 31, 7651.
21. Shi, G.; Zhang, J.; Cao, Y.; Hong, J. *J Makromol Chem* 1993, 194, 269.
22. Hammami, A.; Spruiell, J.; Mehrota, A. K. *Polym Eng Sci* 1995, 35, 797.
23. Hieber, C. A. *Polymer* 1995, 36, 1455.
24. Tiganis, B. E.; Shanks, A.; Long, Y. *J Appl Polym Sci* 1996, 59, 663.
25. Chin, S. C.; Xu, C. A. *Polym Int* 1997, 44, 95.
26. Kim, Y. C.; Kim, C. Y.; Kim, S. C. *Polym Eng Sci* 1991, 31, 1009.
27. Minkova, L. I.; Paci, M.; Pracella, M.; Magagnini, P. *Polym Eng Sci* 1992, 32, 57.
28. Fillon, B.; Wittmann, J. C.; Lotz, B.; Thierry, A. *J Polym Sci, Polym Phys Ed* 1993, 31, 1383.
29. Fillon, B.; Thierry, A.; Lotz, B.; Wittmann, J. C. *J Therm Anal* 1994, 42, 721.
30. Kinsinger, J. B.; Hughes, R. E. *J Phys Chem* 1959, 63, 2002.
31. Li, J. X.; Cheung, W. L. *Demin, J. Polymer* 1999, 40, 1219.
32. Ziabicki, A.; Alfonso, G. C. *Colloid Polym Sci* 1994, 272, 1027.
33. Alfonso, G. C.; Ziabicki, A. *Colloid Polym Sci* 1995, 273, 317.
34. Carfagna, C.; De Rosa, C.; Guerra, G.; Petraccone, V. *Polymer* 1984, 25, 1462.
35. Janimak, J. J.; Cheng, S. Z. D.; Giusti, P. A.; Hsieh, E. T. *Macromolecules* 1991, 24, 2253.
36. Blundell, D. J.; Keller, A.; Kovacs, A. J. *J Polym Sci, Part B: Polym Phys* 1966, 4, 481.
37. Feng, Y.; Jin, X. *J Appl Polym Sci* 1999, 72, 1559.
38. Guerra, G.; Petraccone, V.; Corradini, P.; De Rosa, C.; Napolitano, R.; Pirozzi, B. *J Polym Sci, Polym Phys Ed* 1984, 22, 1029.
39. Pukánszky, B.; Mudra, I.; Stanieck, P. *J Vinyl Add Technol* 1997, 3, 53.
40. Marco, C.; Gómez, M. A.; Ellis, G.; Arribas, J. M., unpublished results.
41. Thierry, A.; Fillon, B.; Straupé, C.; Lotz, B.; Wittmann, J. C. *Progr Colloid Polym Sci* 1992, 87, 28.
42. Fillon, B.; Lotz, B.; Thierry, A.; Wittmann, J. C. *J Polym Sci, Polym Phys Ed* 1993, 31, 1395.
43. Varga, J. in *Polypropylene. Structure, Blends and Composites; Vol. 1, Structure and Morphology*, Karger-Kocsis, J., Ed., Chapman and Hall: London, 1995.
44. Nagarajan, K.; Levon, K.; Myerson, A. S. *J Therm Anal Calorim* 2000, 59, 497.
45. Aboulfaraj, M.; Ulrich, B.; Danoun, A.; G'Sell, C. *Polymer* 1993, 34, 4817.
46. Samuels, R. J. *J Appl Polym Sci* 1975, 13, 1417.
47. Petraccone, V.; Guerra, G.; De Rosa, C.; Tuzi, A. *Macromolecules* 1985, 18, 813.
48. Yadav, Y. S.; Jain, D. C. *Polymer* 1986, 27, 721.